Challenges in Measurement of Broadband THz Photoconductive Antennas

Zach Uttley[1], Jose Santos Batista[1], Mahmudul Doha[3], Katie Welch[2], Hugh Churchill[2,3], and Magda El-Shenawee[1]

[1]Department of Electrical Engineering, University of Arkansas, Fayetteville, AR 72701

[2]Material Science and Engineering Program, University of Arkansas, Fayetteville, AR 72701

[3]Physics Department, University of Arkansas, Fayetteville, AR 72701

***Abstract* — This work utilizes an open bench time-domain spectroscopy system to measure the THz pulse and spectrum of photoconductive antennas (PCAs) with two different active layer materials: low temperature gallium arsenide (LT-GaAs) and 2D black phosphorous (BP). COMSOL Multiphysics modeling of the PCAs has shown that using BP as an active layer greatly increases the optical to THz conversion efficiency compared to LT-GaAs. However, the fabrication and measurement of both devices has demonstrated the opposite.**

***Index Terms* — THz time-domain spectroscopy, photo conductive antennas, black phosphorus, femtosecond laser, COMSOL, electron-beam lithography.**

I. Introduction

As wireless communications, medical imaging, spectroscopy, security, and many other industries continue to expand their needs into higher frequencies, the technology supporting them must advance as well [1-5]. The need for high bandwidth data transfer plays a pivotal role in wireless communications and IOT. The terahertz (THz) frequency band has seen major growth in research in the past decade and has shown the potential to play a role in these fields. The work presented here focuses on challenges in measurement of broadband photoconductive antennas (PCAs) operating in the THz band (~0.1 - 4 THz). The PCAs, described below, are fabricated on low temperature gallium arsenide (LT-GaAs) substrate using electron beam lithography (EBL) and thermal evaporation of chromium/gold (Cr/Au) to form dipole antennas with bowtie shaped electrodes for the purpose of increasing the bandwidth. The same design is used to fabricate emitter device using black phosphorus (BP) as an active layer to further increase the optical to THz conversion efficiency.

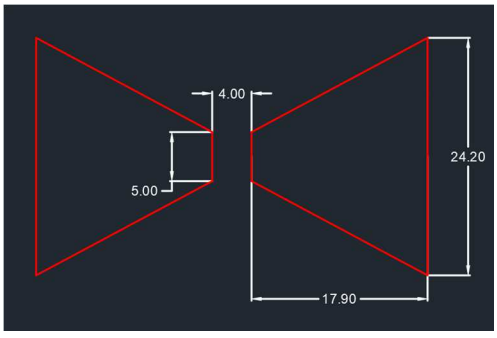

Fig. 1. Dimensioned drawing showing the critical dimensions of the THz PCAs. The 4x5 µm gap is vital for this design.

II. PCA Design and Function

The geometry of the antenna electrodes is best described as trapezoidal with base of 24.2 µm, top width of 5 µm, and height of 17.9 µm. The two electrodes have their short ends facing each other at a spacing of 4 µm (antenna gap) as shown in Fig.1. Sufficiently long and thin transmission lines electrically connect the bias voltage to the antenna. The electrodes and transmission lines are formed with a Cr/Au stack with a thicknesses of 5/50 nm, respectively.

The LT-GaAs material stack starts with 350 µm semi-insulating undoped GaAs substrate, followed by a 50 nm epi grown unintentional doping (UID) GaAs buffer later, finished with a 250 nm UID LT-GaAs layer grown at 250 C and annealed for 10s at 525 C as shown in Fig. 2. The purpose for using the low temperature grown GaAs is to increase the semiconductors mobility and achieve sub-picosecond carrier lifetime to generate THz pulses. The BP material stack begins with a high resistivity silicon wafer followed by a silicon dioxide layer for the antenna to be fabricated on. To lay a single flake of BP onto the PCA gap, the antenna must be etched into

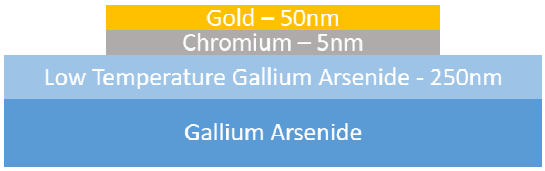

Fig. 2. Material stack for THz PCAs fabricated using LT-GaAs as an active layer.

Fig. 3. Material stack for THz PCAs using BP as an active layer. The metallic electrodes made of Cr/Au are shown inset into the oxide layer of the substrate

978-1-6654-7494-8/23/$31.00 ©2023 IEEE

the oxide layer to create a smooth top surface. In addition to this, the BP is pacified with a capping layer of hexagonal boron nitride (hBN) as shown in Fig. 3.

THz emission is generated through the excitation of photocarriers by a 780 nm femtosecond laser pulse incident on the PCA gap. The laser excites photocarriers within the photoconductive substrate, which are accelerated in the applied DC bias field, generating a photocurrent to drive the antenna, which then emits the THz electric field pulse [6].

In parallel to LT-GaAs, identically dimensioned PCA using the new 2D material black phosphorus (BP) as an active layer

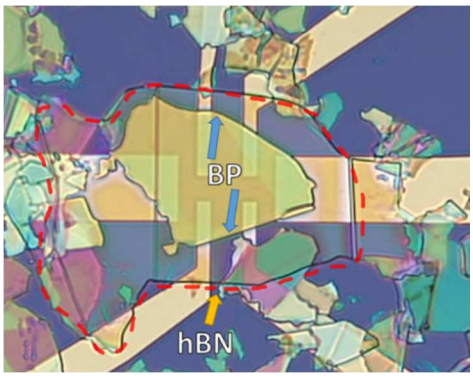

Fig. 4. Hall Bar measurement setup showing the EBL patterned electrodes onto which a BP flake, followed by an hBN passivation layer are laid.

to increase the optical to THz conversion efficiency are being fabricated. BP has been reported to have an extremely high hole mobility of up to 5000 cm^2/Vs while still maintaining a sub picosecond carrier lifetime reported as low as 0.36ps [7-8]. This

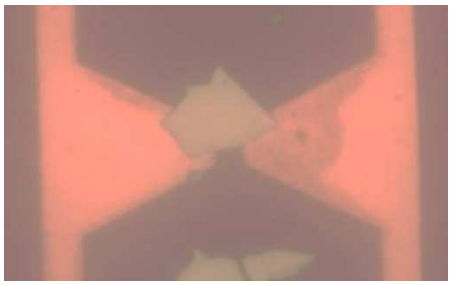

Fig. 5. Hall Bar measurement setup showing the EBL patterned electrodes onto which a BP flake, followed by an hBN passivation layer are laid.

process is much more time consuming than the LT-GaAs devices, as it requires bulk BP exfoliation, multiple flake transfers, passivation to prevent oxidation of the BP, as well as an added etch step to inset the antenna electrodes into the semiconductor substrate (SiO_2). It has been found that the mobility of BP varies between different bulk crystals, requiring the use of hall bar measurements to verify a sufficiently high mobility before fabricating a device. The hall device consists of a BP flake laid over EBL patterned gold electrodes, passivated by a flake of Hexagonal Boron Nitride (hBN) as seen in Fig. 4. Once a flake from the bulk BP crystals mobility has been verified through hall measurements, the flake transfer process can begin, which takes a single BP flake and lays it over the gap of the bowtie PCA fabricated on Silicon Dioxide (SiO_2) as shown in Fig. 5. In this case the BP is now acting as the active photoconductive layer, as opposed to LT-GaAs.

III. Methodology

The measurement and characterization of the THz PCAs is realized using an open-bench time-domain spectroscopy system developed as shown in Fig. 6. The heart of this system is the 780 nm femtosecond laser which can produce a pulse with sub-picosecond width (~ 92 fs). The laser emission is split, polarized, and pulse-conditioned using a group velocity dispersion delay setup (GVD), allowing for the compression or expansion of the pulse width. The system uses computer-controlled delay lines to ensure that the emitted THz pulse and the femtosecond laser beam reach the detector antenna at precisely the same time. Although not specified in the diagram, the detector is a commercial LT-GaAs bowtie antenna developed by TeraView, the geometry of which is protected by intellectual property restrictions. The alignment of the laser beam to both emitter and detector gaps is handled manually using a pair of stacked Elliot stages that independently control the alignment of the incoming laser to each PCA, as well as the THz pulse from emitter to detector. This setup allows for real-time measurements of the THz pulse and spectrum with a viewing window of ~40 ps. The window width is defined by a fast delay line consisting of a galvanometer controlled oscillating rhomboid (RSDL). Note that the 40ps viewing window does not represent the pulse width, which is roughly 3-4 ps wide as shown in Fig. 7. The speed of amplitude of the oscillations directly controls the width and scan rate of the window for measurements. In Fig. 6, the top diagram shows the optical setup. The red beam path represents the initial beam from the femtosecond laser. The pulse is conditioned in the GVD, before meeting a 50/50 beam splitter as shown. From there the beam is separated into an emitter path (green), and a detector path (yellow). The left-most slow delay adds the ability to change the path length on the emitter side, but in general use does not move. The combination of the RSDL and right-most slow delay allows for a ~40 ps viewing window which can be positioned at any point on the ~800ps slow delay line. The bottom diagram shows the THz setup after the fiber ports. From here both beams are aligned to the emitter (green) and detector (yellow), using the alignment stages labeled. The incident power of the laser at the PCA (emitter) is 6 mW, while the detector is fed with an incident power of 5 mW, both of which can be adjusted using attenuators placed before the fiber ports (not shown). The golden ellipsoidal mirrors direct the emitted THz signal such that it will pass through a pinhole placed in the mount labeled “pinhole”. This is a simplified diagram of the measurement setup that does not show multiple half-wave plates used for adjusting the polarization the beam.

A key aspect of the PCA measurements is the alignment of the THz pulse. Alignment is extremely sensitive not only to

978-1-6654-7494-8/23/$31.00 ©2023 IEEE

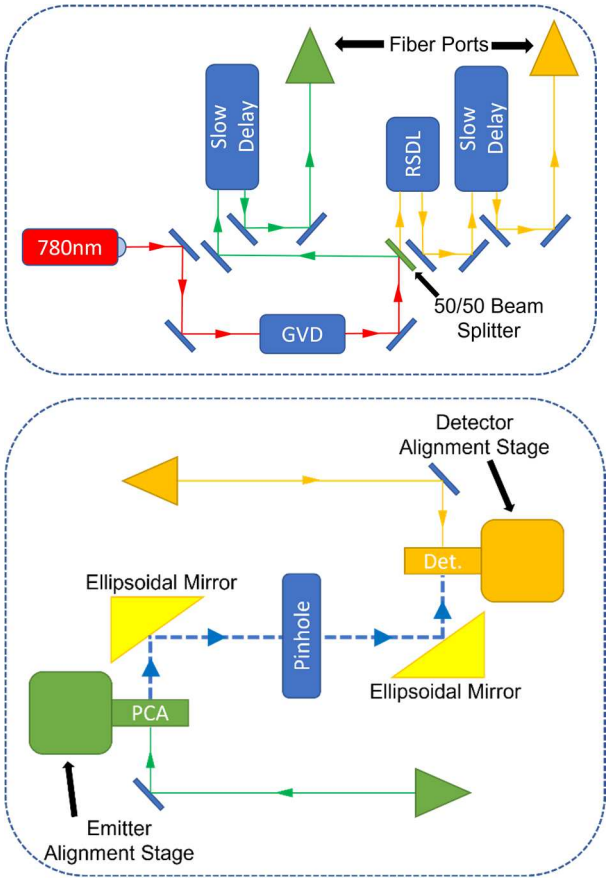

Fig. 6. Top diagram shows the optical side of the TeraAlign measurement setup, including mentioned RSDL and GVD. Bottom shows the alignment side of system, connected to the optical side through single-mode fiber ports.

small adjustments in stage and delay line position, but also to temperature and humidity, making it important to ensure that the conditions under which measurement are taken remain consistent. During measurements, it is challenging to simply view a pulse and confirm that the main contribution is a THz signal. To verify the alignment of the system, brass pinholes are placed directly in the signal path. These pinholes filter low-frequency components out of the pulse, allowing passage for the high frequency component, i.e., THz. It has been observed that when placing a 1 mm diameter brass pinhole (cutoff frequency of ~0.175 THz) in the signal path, one can expect a drop in overall amplitude anywhere from 50-70 percent. If the 1mm pinhole is replaced with one of 0.5 mm diameter (cutoff frequency of ~0.351 THz), another drop of 50-70 percent will be seen. This simple tool is very effective in ensuring that alignments are consistent over many PCAs' measurements. While fabrication quality can play a role in the performance of the final device, alignment is by far the most critical and challenging step in the ensuring quality measurement data.

IV. Results and Discussion

The results so far from the fabrication and measurements of LT-GaAs PCAs with the dimensions/design from Figs. 1-2 have been experimentally shown to produce pulses like commercial THz PCAs currently being used in industry. It should be noted that current efforts are being taken to investigate the cause of unwanted low frequency components being emitted from the proposed THz PCAs, as they take away from the overall optical to THz efficiency of the device.

In Fig. 7, the results of three measurements of the same THz PCA can be seen. From top to bottom, the plots show the THz pulse through air (free space), then through a 1 mm brass pinhole, and finally through a 0.5 mm brass pinhole. It should be noted that the spectrum in each of these cases is obtained through a fast Fourier transform of the time domain pulse then normalized to its maximum to better highlight the effect of the pinhole. The lowest end of the spectrum in the bottom two plots can be seen rolling off due to the pinhole. The spectrum from ~0.1 – 4 THz remains relatively constant in all plots, verifying the alignment of the THz signal from emitter to detector. Furthermore, the peak-to-peak amplitude of the top measurement is ~60 a.u., while the 1 mm and 0.5 mm pinhole measurements are ~18 and ~6 respectively. This gives a signal drop of ~70% from air to 1 mm pinhole, and ~67% from 1 mm to 0.5mm pinhole.

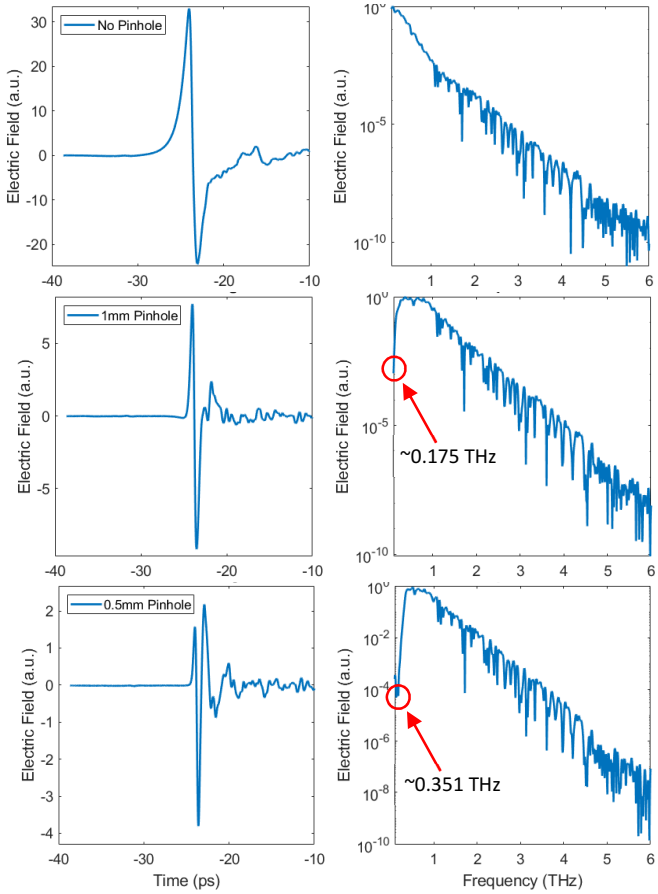

Fig. 7. Experimental measurements of bowtie THz PCA. Top image showing measurement through air. Middle image showing same measurement through 1mm pinhole. Bottom image again showing same measurement but now through 0.5mm pinhole. All measurements taken using same alignment

978-1-6654-7494-8/23/$31.00 ©2023 IEEE

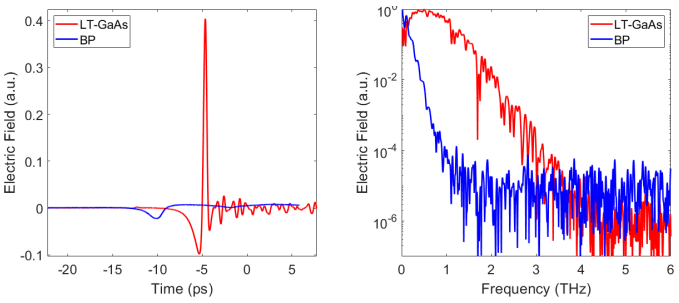

Fig. 8. Measurement of LT-GaAs (red) as compared to the same design PCA with a BP active layer (blue). The spectrum of the BP can be seen to contain very little THz components.

The fabrication and measurement of both LT-GaAs and BP THz PCAs is motivated by extensive computational modeling of these PCAs using COMSOL Multiphysics. Modeling has shown that there should be a substantial increase in signal strength when using BP over LT-GaAs at the same incident laser power, these results are reported in Fig. 2.12 in [9] and Fig. 5 in [10]. Detailed setup of each modeling case is explained in [11]. It should be noted that the COMSOL model did not consider the exact measurement setup (i.e., lenses, mirrors, etc.) but simulated the PCA configuration alone due to computational limitations.

Preliminary comparisons of the two materials is presented in Fig. 8 to experimentally show the current state of BP as compared to LT-GaAs. To verify the increase in optical to THz conversion efficiency when using BP as compared to the conventional LT-GaAs PCAs, as the model in [9-10] has shown, further fabrication and measurements are underway.

V. Conclusion

The results of this work show that the performance of the PCA design presented here when fabricated using LT-GaAs can produce quality THz pulses with a bandwidth of up to 4 THz. The alignment of the TPS system is critical to ensure consistent, quality measurements of each device. The alignment verification process utilizes brass pinholes which pass the THz signal through, filtering the low frequency components from the signal. This effect can be seen in Fig. 7 where the low frequency components of the signal drop off as the diameter of the pinhole decreases.

The COMSOL Multiphysics modeling that preceded these results predicted that fabricating the same emitter devices using BP as the active layer would increase the conversion efficiency of the signal, i.e., converting more of the laser power into a THz electric field [6-7]. However, the initial fabrication and measurement trials of BP THz PCAs have shown that not only is the pulse much weaker, but the spectrum experiences a sharp drop off beginning at ~0.1 THz that quickly decays to the system noise level around 1 THz. Overall, improving the PCAs efficiency using BP as an active layer has not been successful so far. The discrepancies of modeled vs. measured BP antennas is believed to be due to the large variation in BP mobility between manufactures and what was reported in the literature [11]. Further work including changes in BP manufacturer, layer thickness, and fabrication process are being taken to realize the goal of creating broadband THz PCAs using BP.

VI. Acknowledgement

The authors would like to acknowledge the National Science Foundation (NSF) funding award #1948255. The Authors acknowledge the help from Prof. Martin Mittendorff and his postdoctoral fellow Dr. Han for measuring the mobility of the LT-GaAs wafers used in this work. The Authors also acknowledge TeraView Ltd at UK for providing the TeraAlign TDS system used in this work.

References

[1] Nathan M. Burford, Magda O. El-Shenawee, "Review of terahertz photoconductive antenna technology," Opt. Eng. 56(1) 010901 (24 January 2017)

[2] H. Tataria, M. Shafi, A. Molisch, M. Dohler, H. Sjoland and F. Tufvesson, "6G Wireless Systems: VIsion, Requirements, CHallenges, Insights, and Opportunities," Proceedings of IEEE, vol. 109, no. 7, pp. 1166-1199, 2021.

[3] Rong, Y., Theofanopoulos, P.C., Trichopoulos, G.C. et al. A new principle of pulse detection based on terahertz wave plethysmography. Sci Rep 12, 6347 (2022).

[4] P. K. Lu, D. Turan, M. Jarrahi, "High-Power Terahertz Generation from Bias-Free Nanoantennas on Graded Composition InGaAs Structures", Optics Express, 30, 1584-1598, 2022

[5] Z. D. Taylor *et al*., "THz Medical Imaging: in vivo Hydration Sensing," in *IEEE Transactions on Terahertz Science and Technology*, vol. 1, no. 1, pp. 201-219, Sept. 2011, doi: 10.1109/TTHZ.2011.2159551.

[6] Burford, N. M. (2016). Design, Fabrication and Measurement of a Plasmonic Enhanced Terahertz Photoconductive Antenna. Graduate Theses and Dissertations Retrieved from https://scholarworks.uark.edu/etd/1841

[7] K. Wang, B. Szydlowska, G. Wang, X. Zhang, J. J. Wang, J. J. Magana, L. Zhang, J. N. Coleman, J. Wang and W. J. Blau, "Ultrafast Nonlinear Excitation Dynamics of Black Phosphorus Nanosheets from Visible to Mid-Infrared," ACS Nano, vol. 10, no. 7, pp. 6923- 6932, 2016.

[8] G. Long, D. Maryenko, J. Shen, S. Xu, J. Hou, Z. Wu, W. K. Wong, T. Han, J. Lin, Y. Cai, R. Lortz and N. Wang, "Achieving Ultrahigh Carrier Mobility in Two-Dimensional Hole Gas of Black Phosphorus," Nano Letters, vol. 16, no. 12, pp. 7768-7773, 2016.

[9] Santos Batista, J. I. (2021). Computational Modeling of Black Phosphorus Terahertz Photoconductive Antennas using COMSOL Multiphysics with Experimental Comparison against a Commercial LT GaAs Emitter. M.S. Thesis , University of Arkansas, ProQuest, 2021.

[10] M. Doha, J. Santos Batista, A. Rawwagah, J. Thompson, A. Fereiodouni, K. Watanabe, T. Taniguchi, M. El-Shenawee and H. Churchill, "Integration of multi-layer black phosphorus into photoconductive antennas for THz emission," Journal of Applied Physics, vol. 128, no. 6, pp. 063104, 2020

[11] J. S. Batista, H. O. Churchill, and M. El-Shenawee, "Black phosphorus photoconductive terahertz antenna: 3d modeling and experimental reference comparison," Journal of the Optical Society of America B, vol. 38, no. 4, p. 1367, 2021.